Materials Science Forum Vol.426-432 (2003) pp.859-864

MECANICAL PROPERTIES OF CEMENTITE AND FABRICATION OF ARTIFICIAL PEARLITE

M. Umemoto, Y. Todaka and K. Tsuchiya

Department of Production Systems Engineering, Toyohashi University of Technology,

Tempaku-cho, Toyohashi 441-8580, Japan

Keywords: Cementite, Pearlite, Deformation, Dissolution, Mechanical Properties, Characterization

Abstract. The deformation behavior of cementite was studied using eutectoid steels with pearlitic and spheroidite structures and fine grained bulk cementite prepared by sintering the mechanically alloyed powders. Cementite lamellae in deformed pearlite exhibited inhomogeneous slip, thinning by deck-of-cards slip, homogeneous bending, fragmentation, cleavage fracture and cracking by shear bands. Complete dissolution of cementite lamellae and spheroidal cementite was also observed in specimens deformed at high strain rates. The polycrystalline bulk cementite is brittle and fractures within elastic limit when deformed below 573 K. However, large plastic deformation was observed when compressed at high temperatures (over 773 K) and low strain rates ($10^{-5} \sim 10^{-3}$ s^{-1}). The artificial pearlite was successfully fabricated by hot compression starting from the alternately stacked cementite and low carbon steel sheets.

Introduction

Cementite is one of the most important phases in steels, which plays a critical role in the mechanical properties of steels. However, the deformation behavior of cementite has not been understood well. Wire drawn pearlite has been studied [1-6] extensively because of the various industrial applications such as tire reinforcement cord or suspension bridge cable. Despite the limited ductility of monoclinic cementite crystals observed in cast iron, the cementite lamellae in pearlitic wire co-deform with ferrite [2,3]. Direct evidences for plastic deformation of cementite due to dislocation gliding has been obtained using transmission electron microscopy (TEM) [1]. It has been recognized that tensile deformation of thick cementite lamella favors brittle failure, whereas compression or drawing and thin cementite favor ductile behavior [2,3]. It has been reported that a substantial proportion of the cementite in pearlite dissolves during deformation at room temperature [4,6]. Complete dissolution of cementite has also been observed in pearlitic steel after ball milling [7] or torsion straining under high pressure [8]. Superplastic deformation was observed in a fine-grained cementite-based composite (80 vol% of cementite) at high temperature [9].

The present study aims to study the deformation behavior of cementite in steels and fine grained bulk cementite in detail and try to find out the relation between the plastic deformation and dissolution of cementite lamellae and superplastic deformation of fine grained cementite.

Experimental Procedures

The eutectoid steels of Fe-0.76C (Fe-0.76C-0.20Si-1.37Mn in mass%) and Fe-0.80C (Fe-0.80C-0.25Si-0.50Mn in mass%) were used. Coarse pearlite was obtained by austenitized at 1273 K for 1.8 ks and transformed to pearlite at 963 K for 43.2 ks. The interlamellar spacing of the pearlite thus obtained was 710 nm. Fine pearlite was obtained by austenitized at 1173 K for 0.9 ks and kept at 893 K for 90 s. The interlamellar spacing of the pearlite thus obtained was 114 nm. Spheroidite structure was obtained by tempering the quenched martensite at 983 K for 79.2 ks. Those specimens were cold rolled with 5 % reduction for every pass to the final reduction in the range 30 ~ 60 %. For the high strain rate deformation, a ball drop experiment was performed. A weight with a ball attached on its bottom was dropped onto the specimens. The specimens used for

a ball drop experiment were fine pearlite produced by air cooling after hot rolling. The interlamellar spacing of the samples was around 100 nm. The microstructural observation of deformed pearlite was conducted by scanning electron microscope (SEM; JEOL JSM 6500F) after etched by 5 % Nital. To fabrication bulk cementite samples, pure Fe, graphite and Mn were mixed at nominal compositions of $Fe_{75}C_{25}$ or $(Fe_{0.95}Mn_{0.05})_{75}C_{25}$, and mechanical alloyed (MA) for 360 ks in a conventional horizontal ball mill with a ball to powder weight ratio of 100 : 1 under the protective Ar atmosphere. The MA powders were subjected to spark plasma sintering (SPS) at 1173 K for 900 s with a stress of 50 MPa. Compression tests were carried out for prism specimens 4 x 4 x 6 mm with constant cross-head speed of 0.5 mm/min (initial strain rate of 1.4 x 10^{-3} s^{-1}) at various temperatures. The microstructures of specimens were observed by SEM and TEM (HITACHI H-800).

Results and Discussion

Deformation of lamellar cementite

The deformation behavior of cementite lamellae was studied using coarse and fine pearlite. Deformation was applied either by cold-rolling or a ball drop test. By etching for a proper period, ferrite lamellae are preferentially etched out for several 100 nm in depth from the polished surface and cementite lamellae can be observed three dimensionally. Fig. 1 shows typical deformed structure of cementite lamellae viewed along the transverse direction (TD) of the rolled pearlitic sample. The rolling direction is parallel to horizontal line in all the pictures. It is seen that cementite lamellae either deform plastically or fracture in a brittle manner. Fig. 1 (a) shows the case that cementite undergoes inhomogeneous plastic deformation by rigid blocks sliding past each other. Slip steps with the height of about 50 nm spaced approximately every 150 nm are clearly observed on the side surface (ferrite/cementite interface before etching). Such slip steps in the cementite are considered to be initiated where narrow slip bands in the ferrite cause locally high stress concentration at the ferrite-cementite interface. It was noticed that the slip steps are more pronounced in cause pearlite than fine pearlite. Fig. 1 (b) shows the case that the cementite lamella was smoothly thinned or necked. This type of deck-of-cards slip will take place when one highly stressed slip system in the ferrite is nearly parallel to the plane of the lamellae. Small slip steps are

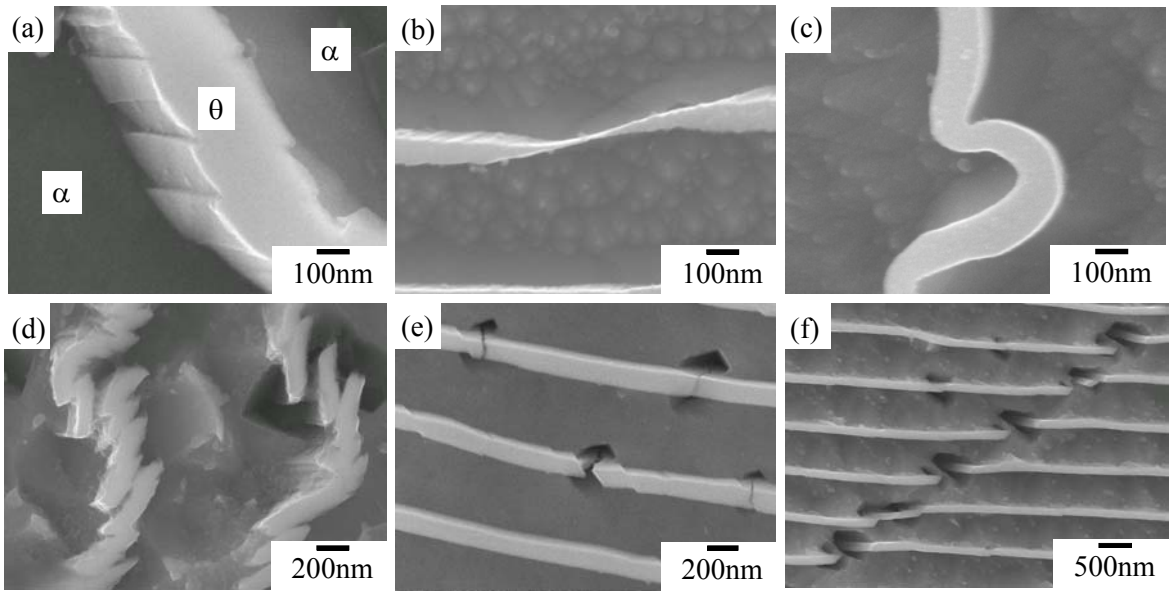

Fig. 1 SEM micrographs showing various deformed morphologies of cementite in pearlitic Fe-0.76C steel after cold-rolled in reduction ((a), (b) 30 %, (c), (d) 60 % and (e), (f) 30 %).

also seen along the entire cementite lamella. Fig. 1 (c) shows the case that cementite lamella bent or buckled severely. The interface appears smooth and suggesting that the cementite plate is deformed homogeneously. Such buckling of lamellae was observed for those oriented nearly perpendicular to the rolling plane. Fig. 1 (d) shows the case of fragmentation of cementite lamellae. Cementite undergoes inhomogeneous plastic deformation by rigid blocks sliding past each other. This seems an extreme case of the deformation shown in Fig. 1 (a). By heavy deformation, the slip distance in cementite lamella exceeded its thickness and cementite plate was separated into small pieces with length less than 500 nm. Fig. 1 (e) shows the cleavage type fracture in cementite lamellae oriented nearly parallel to the rolling plane. The tensile stress produced by rolling is considered to be responsible for these cracks. The plane of fracture is not flat but rather irregular and nearly perpendicular to the ferrite/cementite interface. The fact that the planes of fracture are often almost perpendicular to the ferrite/cementite interface corresponds well with the angle between the reported cleavage planes of cementite ($\{110\}_\theta$, $\{100\}_\theta$ and $\{210\}_\theta$) [10] and cementite habit plane ($(001)_\theta$) [11]. The ferrite areas around the cracks of cementite lamellae are sensitive for etching and appear as holes after etching. Fig. 1 (e) shows fracture of cementite plates by shear bands which are inclined about 30 degree to rolling direction. This type of fracture by shear bands is observed only in coarse pearlite. At shear bands in fine pearlite, the cementite lamellae become thin but never rapture.

Another type of structural change in pearlite by deformation was observed in the specimen subjected to a ball drop experiment. Fig. 2 shows the area near the surface of the pearlitic specimen after a ball drop experiment (dropped 8 times with 5 kg in weight and 1 m in height). The upper part of Fig. 2 (a) shows a uniform contrast structure and the bottom part shows the deformed pearlite structure. The boundaries between the two regions are sharp and clear. The enlarged picture of the homogeneous structure (Fig.2 (b)) region shows randomly distributed a large number of very fine curved white lines with less than 20 nm in length. According to the TEM observation, the grain size of ferrite of this region is less than 100 nm and cementite is completely dissolved. Thus the fine lines in Fig. 2(b) probably correspond to the grain boundaries of nanocrystalline ferrite. The hardness of this region is extremely high around 11 GPa. Fig. 2 (c) is the enlarged picture of region (c) in Fig. 2 (a). Deformed pearlite similar to that observed in a rolled specimen is seen. The hardness of this region is less than 7 GPa. These results indicate that cementite lamellae are deformed in certain extent before dissolution and there is a critical deformed state in pearlite to change into nanocrystalline structure.

Fig. 3 shows the dissolution of spheroidal cementite particles by a ball drop experiment (dropped 8 times with 5 kg in weight and 1 m in height). The middle part of Fig. 3 (a) shows a layer of uniform structure and upper and bottom parts show spheroidite structure. The enlarged picture of the homogeneous structure (Fig. 3 (b)) shows similar morphology with Fig. 2 (b). From TEM observation, it is confirmed that this region is nanocrystalline ferrite structure and cementite particles are completely dissolved. Fig. 3 (c) is the enlarged picture taken just outside of the

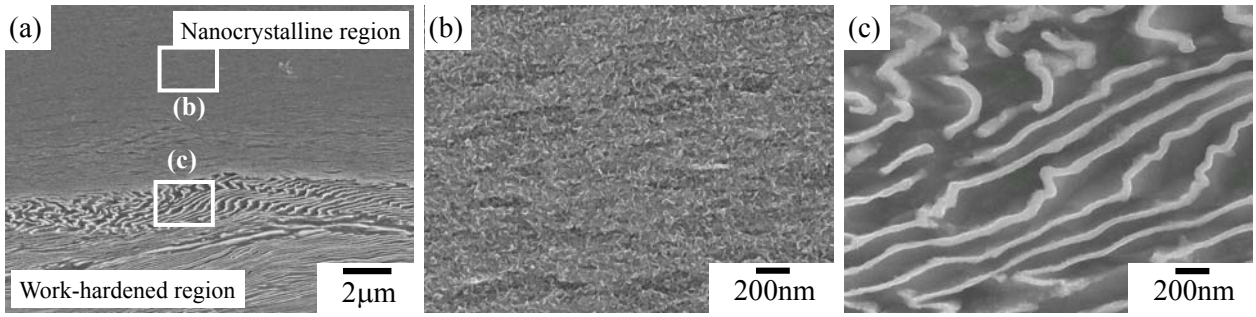

Fig. 2 SEM micrographs showing dissolution of cementite in pearlitic Fe-0.80C steel by ball drop deformation at room temperature (dropped 8 times from 1 m height with 5 kg weight). (a) low magnification, (b) high magnification of nanocrystallized region and (c) high magnification of work-hardened region.

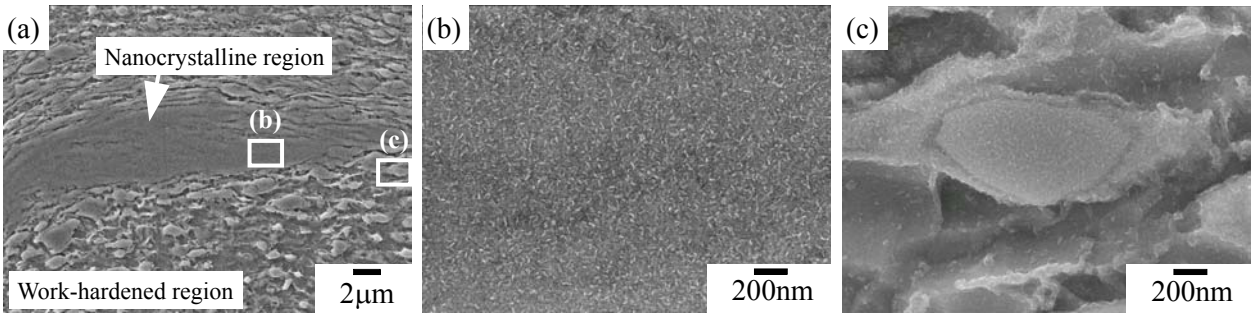

Fig. 3 SEM micrographs showing dissolution of cementite in Fe-0.80C steel with spheroidite structure by ball drop deformation at room temperature (dropped 30 times from 1 m height with 5 kg weight). (a) low magnification, (b) high magnification of nanocrystallized region and (c) high magnification of cementite near homogeneous structure region.

homogeneous structure region (marked (c) in Fig. 3 (a)). The cementite particle surrounded by nanocrystalline ferrite looks not deformed. It is interesting to note that after severe deformation of spheroidite by a ball drop test, cementite particles are either dissolved completely or maintain their original shape. No intermediate state of cementite particles was observed. This indicates the possibility of diffusionless transformation in the cementite dissolution by deformation.

The partial or complete dissolution of cementite by severe plastic deformation has been observed previously [4,6,7,12]. Two mechanisms of cementite dissolution have been proposed. One [13] is based on the binding energy between carbon and dislocation in ferrite and another [6] is based on the interfacial energy of ferrite/cementite. However, these mechanisms cannot explain the observed results that the large cementite particles around half micron can dissolve or dissolution occurs in a significantly short time. Further investigations are required to understand the mechanism of cementite dissolution by deformation. It can be suggested that complete dissolution of cementite is associated with the nanocrystallization of ferrite and a large deformation at high strain rate is favorable condition for the dissolution of cementite.

Deformation of bulk cementite and fabrication of artificial pearlite

The flow curves of bulk cementite ($(Fe0.95Mn0.05)_3C$) obtained by compression test were show in Fig. 4 [14]. As seen, no ductility was observed at room temperature (RT) so that the real yield strength was not found. At 573 K, however, a little elongation was observed and tensile strength was found to be lager than 3.2 GPa. Large plastic deformation was observed above 773 K. The flow stress at 973 K becomes extremely small accompanying large ductility. The strain rate sensitivity exponent measured at 973 K was 0.41, close to the value of 0.5 around that superplasticity is observed generally.

Kim *et al* [9] have been reported that a fine-grained cementite base material exhibits superplastic properties. They prepared a fine-grained (linear intercept grain size of 2.1 μm) material contains 80 vol% cementite from gas atomized powder. It is expected that the present bulk cementite may exhibit superplastic flow since the grain size (linear intercept grain size is 0.41 μm) is much smaller than theirs. A preliminary compression test was carried out at 973 K and 100 MPa. Fig. 5 shows a specimen before and after the compression deformation. The initial height of the specimen was 5.3 mm and a final height was 0.76 mm. The obtained

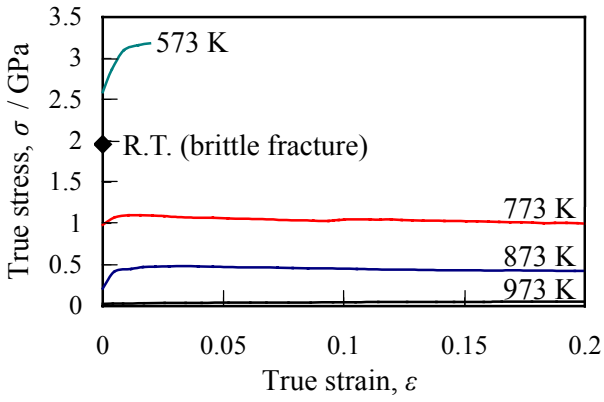

Fig. 4 Compressive stress-strain curves of $(Fe_{0.95}Mn_{0.05})_3C$ at various temperatures.

compression strain is -1.94 and this is equivalent to a tensile elongation of 600 %. In spite of such a large deformation, no cracks were observed either on the surface or in the interior of the material. The hardness of the sample at room temperature did not change by this deformation and maintained the initial hardness of 12 GPa. The change in grain shape by plastic deformation was examined by SEM observation viewed parallel to the compression axis. The aspect ratio measured in the specimen compressed 85 % was 0.800 which is far larger than the calculated value of 0.058 assuming homogeneous deformation. The TEM observation from the compression direction revealed clear grain growth from 0.46 to 1.5 μm as shown in Fig. 6. Dislocations are scarcely observed in the grains after compressed to the strain of -1.94. From these observations, it can be concluded that the present fine grained bulk cementite specimen deforms at 973 K and 100 MPa mostly by grain-boundary sliding mechanism and partly by a slip deformation mechanism. Recently it has been reported that after heavy deformation by wire drawing of pearlite, lamellae cementite turns out to be nanocrystals [4-6]. This suggests that grain boundary sliding is a possible deformation mechanism of cementite lamellae in heavily deformed pearlite.

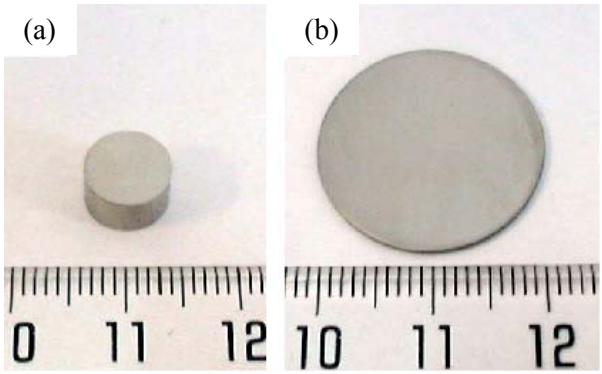

Fig. 5 $(Fe_{0.95}Mn_{0.05})_3C$ specimen (a) before and (b) after compressive deformation at 973 K with the initial stress of 100 MPa. (a) Diameter: 8.0 mm, Thickness: 5.3 mm, (b) Diameter: 21.0 mm, Thickness: 0.76 mm.

It has been known that lamellar structure of fine pearlite is maintained even after severe deformation [2-6]. Detailed observation revealed that the cementite lamellae fragmented into planar arrays of small particles [4-6]. This polycrystallization of cementite may assist the uniform deformation of cementite and ferrite in pearlite. To examine the cooperative deformation of cementite with ferrite, bulk cementite sheet samples were deformed with low carbon steel sheets using the SPS equipment. Cementite disks of 6 mm in diameter and 0.45 mm thick and low carbon

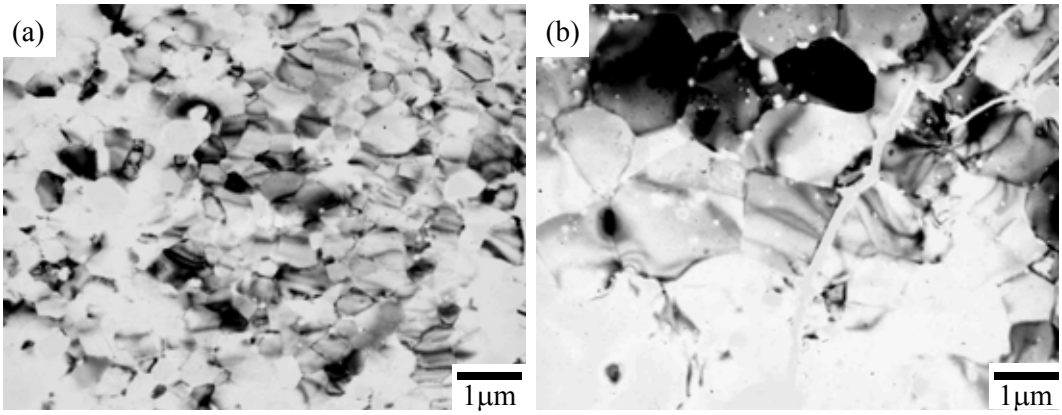

Fig. 6 TEM micrographs of $(Fe_{0.95}Mn_{0.05})_3C$ (a) before and (b) after compression at 973 K with the initial stress of 100 MPa. The height of specimen reduced from 4.2 mm to 0.89 mm.

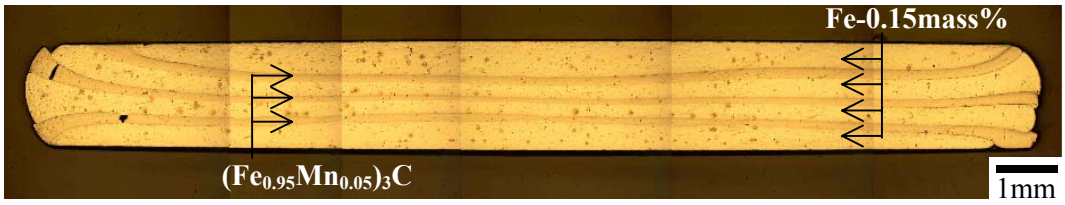

Fig. 7 Cementite/low carbon (Fe-0.15mass%C) steel multilayers produced by compression at 873 K with the initial stress of 100 MPa.

(Fe-0.25mass%C or Fe-0.15mass%C) disks of 6 mm in diameter and 0.90 mm in thickness were stacked alternately. After stacking, the sample was deformed with compression at 873 K and 100 MPa. The result is shown in Fig. 7 where 3 layers of $(Fe_{0.95}Mn_{0.05})_3C$ and 4 layers of fine grained (about 1 μm) Fe-0.15mass%C steel disks were compressed to 66 % in reduction. It is seen that both low carbon steel and cementite deformed uniformly and constructed a structure of cementite-ferrite multi-layers (artificial pearlite).

Summary

The deformation behavior of cementite was studied. In rolled pearlite, cementite lamellae showed inhomogeneous slip, thinning or necking by deck-of-cards slip, homogeneous bending, fragmentation, cleavage fracture and cracking by shear bands. The plastic deformability of cementite lamellae increased with decreasing thickness. The fracture of cementite or void formation is scarcely observed in fine pearlite. Complete dissolution of cementite lamellae was observed in eutectoid specimens deformed by a ball drop experiment. The dissolution of cementite is always accompanied by the nanocrystallization of ferrite. A large deformation at high strain rate is considered to be a favorable condition for the dissolution of cementite lamellae.

In spite of the brittle behavior of bulk cementite at temperatures below 373K, high deformability was observed when compressed at high temperature (over 773 K) and low strain rate ($10^{-5} \sim 10^{-3}$ s^{-1}). The dislocation free structure and high strain rate sensitivity exponent suggested the possibility of superplastic deformation of bulk cementite due to fine grained structure. It was shown that the fine grained bulk cementite sheets co-deform uniformly with low carbon steel sheets. It was demonstrated that artificial pearlites with arbitrary interlamellar spacing can be produced.

Acknowledgement

This study is partly supported by the Grant-in-Aid by the Japan Society for the Promotion of Science (No.14205103).

References

[1] A.Inoue, T.Ogura and T.Masumoto: Trans. JIM. Vol.17 (1976), p.149.
[2] G.Langford: Metall. Trans. Vol.8 (1977), p.861.
[3] D.A.Porter, K.E.Eastering and G.D.W.Smith: Acta Metall. Vol.26 (1978), p.1405.
[4] M.H.Hong, W.T.Reynolds, Jr., T.Tarui and K.Hono: Met. Mater. Trans. Vol.30A (1999), p.717.
[5] S.Tagashira, K.Sakai, T.Furukawa and T.Maki: ISIJ Int. Vol.40 (2000), p.1149.
[6] J.Languillaume, G.Kapelski and B.Baudelet: Acta mater. Vol.45 (1997), p.1201.
[7] Y.Xu, M.Umemoto and K.Tsuchiya: Mater. Trans. Vol.43 (2002), p.2205.
[8] A.V.Korznikov, Y.V.Ivanisenko, D.V.Laptionok, I.M.Safarov, V.P.Pilyugin and R.Z.Valiv: NanoStructured Mater. Vol.4 (1994), p.159.
[9] W.J.Kim, J.Wolfenstine, O.A.Ruano, G.Frommeyer and O.D.Sherby: Metall. Trans. Vol.23A (1992), p.527.
[10] A.Inoue, T.Ogura and T.Masumoto: Trans. JIM Vol.17 (1976), p.664.
[11] W.Pitch: Acta Cryst. Vol.10 (1962), p.79.
[12] Y.Todaka, M.Umemoto and K.Tsuchiya: ISIJ Int. Vol.42 (2002), p.1430.
[13] A.A.Bataev, V.I.Tushinskii and V.A.Bataev: Phys. Met. Metallography Vol.80 (1995), p.580.
[14] T.Terashima, T.Suzuki, Y.Tomota and M.Umemoto: CAPM ISIJ (2003) in press.